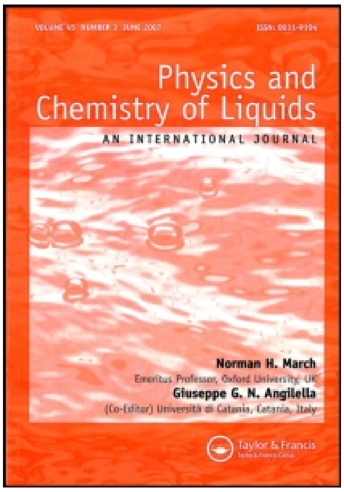

Physics and Chemistry of Liquids
Publication details, including instructions for authors and subscription information:
http://www.informaworld.com/smpp/title~content=t713646857

Some Aspects of Phase Diagrams of Homonuclear Diatomic Assemblies, Including Melting and Critical Point Properties

N. H. March[a]; M. P. Tosi[a]
[a] Istituto Nazionale di Fisica delta Materia and Classe di Scienze, Scuola Normale Superiore, Pisa, Italy

To cite this Article March, N. H. and Tosi, M. P.(1997) 'Some Aspects of Phase Diagrams of Homonuclear Diatomic Assemblies, Including Melting and Critical Point Properties', Physics and Chemistry of Liquids, 35: 3, 131 — 151
To link to this Article: DOI: 10.1080/00319109708030582
URL: http://dx.doi.org/10.1080/00319109708030582

Phys. Chem. Liq., 1997, Vol. 35, pp. 131–151
Reprints available directly from the publisher
Photocopying permitted by license only

Review

SOME ASPECTS OF PHASE DIAGRAMS OF HOMONUCLEAR DIATOMIC ASSEMBLIES, INCLUDING MELTING AND CRITICAL POINT PROPERTIES

N. H. MARCH and M. P. TOSI

Istituto Nazionale di Fisica della Materia and Classe di Scienze,
Scuola Normale Superiore, I-56126 Pisa, Italy

(Received 21 February 1997)

Some aspects of the phase diagrams are considered for the homonuclear diatomics H_2, N_2, O_2 and the halogens I_2, Br_2 and Cl_2. It is first pointed out that, at the critical point, N_2 and O_2 resemble argon, while H_2 has common elements with He.

Attention is focussed on similarities between H_2 and I_2, and the halogens Br_2 and Cl_2 under pressure, though it is stressed that totally different ranges of pressure are involved when comparing these materials. However, zig-zag chains appear to play a role in the solid-state structures of all these materials, and these lead to two-dimensional structures, and correspondingly low melting points, with increasing pressure.

After a survey of some further facts on crystal transitions under pressure, model predictions plus computer experiments are invoked. Some possible directions for future progress are proposed.

Keywords: High pressures; insulator-metal transitions; orientational correlations

CONTENTS

1. BACKGROUND AND OUTLINE

Elements which, when condensed, lead to monatomic dense phases, have phase diagrams [1] which by now are fairly well understood, at least at a semiquantitative level. Typically, one might take the condensed rare gases, Ar, Kr, and Xe which have insulating properties over a wide range of pressure and temperature, though Xe is known to eventually exhibit an insulator-metal transition under extreme thermodynamic conditions. Or one may also single out simple conducting phases of the alkali metals Na and K, though the heavier members of this series Rb and Cs exhibit remarkable structural properties along the liquid-vapour coexistence curve towards the critical point [2].

But when one turns to elemental systems in which, under ordinary conditions of temperature and pressure, chemical bonding plays a central role, the situation as to phase diagrams [3] is less well understood, though considerable progress has been made over the last two decades. As examples, we may cite the diatomic molecular assemblies H_2, N_2, O_2 and the halogens I_2, Br_2 and Cl_2 and these materials will be the focus of all attention in this review.

Before briefly outlining the content of this article, a short discussion is called for concerning the inclusion of condensed O_2. It is different from the other homonuclear diatomic molecules considered here, due to the presence of two unpaired electron spins residing on each molecule. As emphasized, for instance, by Meier *et al.* [4] the interplay of the spin-independent and the magnetic exchange interactions should have its influence on the phase diagram. Indeed, one of the consequences is that the low-temperature α-phase is a single-element insulating antiferromagnet. We simply record here that, as a consequence of measurements of magnetization as a function of pressure p[5] and neutron scattering investigations [6] (see also [7]), a consistent picture of the magnetic excitations can be constructed. We shall return to solid O_2 in the penultimate section of this article.

As to the content of the remainder of the review, it will prove useful in section 3 below to survey critical point properties when available, and to make some groupings among the substances considered, and also to relate to monatomic systems briefly. Melting and orientational disorder will then be discussed, with some emphasis given initially to computer simulation and modelling. Fluid oxygen has interesting optical behaviour and this will be summarized. Should zig-zag chains, prominent at lower pressures in the phase diagram of solid I_2, persist as the temperature is raised, some phenomenology is presented to relate melting and orientational disordering temperatures.

Structural properties of the solid halogens under pressure, and useful scaling rules, including insulator-metal transitions, will be reviewed. In the penultimate section, orientational ordering in solid H_2 will be one focal point, and then the way the phase boundaries near $T=0$ are affected by elementary excitations will be considered. The article concludes with a brief summary and some remarks about unresolved issues.

A valuable general reference to work on molecular solids under high pressure is the article by Ross and McMahan [8].

2. PRIMITIVE PHASE DIAGRAM OF HYDROGEN: SOME SALIENT FEATURES

Leung *et al.* [9], in early work, constructed a primitive phase diagram for hydrogen. Of course, the details of this have been much enriched, and certain features modified semiquantitatively in the intervening period. Their diagram was built up by using, in addition to the then available experimental data, empirical rules and extrapolation formulas.

One empirical rule, the Herzfeld criterion for the insulator-metal transition [10] will be referred to again later in the present article in the context of the solid halogens. It is now known that this transition, as sketched in Figure 1 which reproduces the phase diagram of Leung *et al.* [9], is moved to somewhat higher pressures. On the logarithmic scale of pressure in Figure 1 the change is small, but the recent work of Weir *et al.* [11] on fluid H_2 and D_2 conjectures that in the cold solid phase the pressure which will be required to induce the metallic phase is ≈ 3.5 Mbar.

We note too the recent path-integral Monte Carlo simulation of dense fluid hydrogen by Magro *et al.* [12]. This shows clearly the transition with increasing temperature from a molecular fluid phase to an atomic fluid. The results of Magro *et al.* have been modelled by the present writers [13] in both atomic and molecular phases by a caged H atom and a caged H_2 molecule. Though the infinite barrier of the caged models is known to overestimate the effects of compression, the gist of the results of Magro *et al.* on the variation of electronic kinetic energy with density is obtained both in the very high temperature atomic fluid and in the lower temperature molecular phase.

Returning to the original construction of Figure 1, Leung *et al.* [9] extrapolated the melting curve of molecular hydrogen well beyond its measured portion. The extrapolated melting curve had the approximate form $p \propto T^{1.78}$, which is quite similar to the melting curve of argon at high temperature (see Stishov [14]).

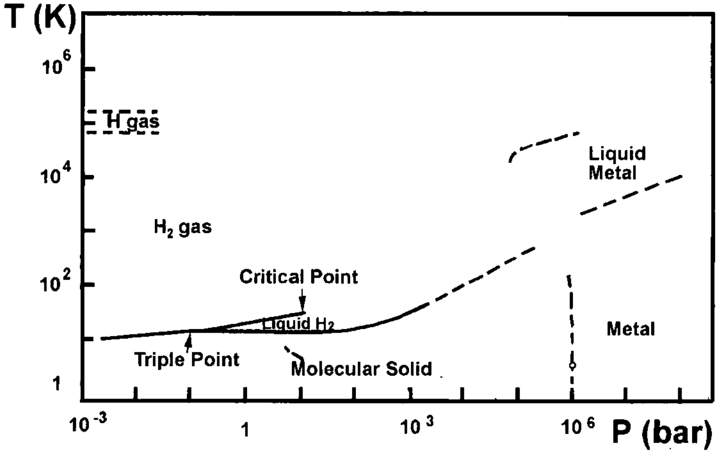

FIGURE 1 Primitive phase diagram for hydrogen (after Leung *et al.* [9]).

Having made these comments on the updating of the phase diagram of Leung *et al.*, we shall begin by collecting data on the homonuclear diatomic molecular assemblies considered below, at their critical points. Such a point for hydrogen is a prominent feature in Figure 1.

3. CRITICAL POINT PROPERTIES OF FLUIDS OF HOMONUCLEAR DIATOMIC MOLECULES

Following the above introduction to some gross features of the phase diagram of H_2 (and D_2 is hardly distinguishable on the scale of Figure 1), let us turn to compare H_2 in its critical point behaviour with those other diatomics of interest here for which relevant data are available.

Very recently, it has been shown [15] that in a final structural theory of the pair distribution function $g(r)$ at the critical point of the heavier rare gases Ar, Kr and Xe, the so-called compressibility ratio $p/\rho k_B T$ must play an important role. Defining the critical compressibility ratio Z_c therefore as

$$Z_c = p_c/\rho_c k_B T_c \;, \tag{3.1}$$

with ρ_c the critical value of the number density etc., the inverse of Z_c is recorded in Table I for some diatomic fluids of interest here, in comparison with rare gas data, from a compilation of Blinder [16].

As indicated below Table I, the point to be emphasized in the present context is the separation between values of Z_c^{-1} for the 'quantal' fluids H_2 and He on the one hand and the 'argon-like' fluids on the other, N_2 and O_2 having virtually the same compressibility ratio $Z_c \approx 0.29$ as the heavier rare gases.

It is relevant here to note that in early work, Guggenheim [17] plotted the liquid-gas coexistence for the substances other than H_2 and He recorded in Table I, using reduced variables T/T_c and ρ/ρ_c. An 'almost' universal curve was obtained, which is reproduced, for example, in Figure 24.11 of the book by Berry *et al.* [18].

The important survey article of Levelt Sengers *et al.* [19] contains in Table 34 critical region parameters for some fifteen fluids. The available data for substances listed in Table I are reproduced from their collected results in Table II below.

4. SOME STRUCTURAL PROPERTIES: ESPECIALLY SOLID HALOGENS, AND THE INSULATOR-METAL TRANSITION INDUCED BY PRESSURE

Pioneering work on the properties of solid I_2 was carried out by Drickamer and coworkers [20]. Their study demonstrated that the electrical resistance of solid I_2 decreases drastically with increasing pressure and exhibits metallic behaviour when $p \approx 20$ GPa. Measurements of optical absorption [21] also demonstrated that the optical gap, having a value of 1.3 eV at atmospheric pressure, tends to zero at around 16 GPa. Subsequent experiments [22] using X-rays showed

TABLE I Inverse Z_c^{-1} of critical point compressibility ratio defined in eqn (3.1) for various fluids composed of diatomic molecules. Fluids of rare gas atoms are also entered, for comparison purposes (data taken from compilation of Blinder [16])

				Substance *					
	H_2	He	:	N_2	O_2	Ar	Kr	Xe	CO^+
Z_c^{-1}	3.05	3.08		3.42	3.42	3.4(3)	3.4	3.4	3.54

*It may be relevant to note that Z_c^{-1} for Ne lies between the 'quantal' systems H_2 and He and the 'argon-like' case, and much nearer to the 'quantal' values (Ne: $Z_c^{-1} = 3.09$). Blinder [16] notes in his tabulation for a wider variety of molecular substances that Z_c^{-1} values can vary over a range from 3 to 5, with an average near to 3.75. The highest value he records is $Z_c^{-1} = 4.99$ for CH_3COOH.

$^+$The value of Z_c^{-1} for CO, which is isoelectronic with N_2, has been entered also in Table I, because of a later comparison between Hugoniots of N_2 and CO.

TABLE II Critical point parameters, p_c in MPa, T_c in K and mass density d_c in kg/m^3 (after Levelt) Sengers *et al.* [19])

	N_2*	O_2	Ar	Kr	Xe	p-H_2*	^3He	^4He
p_c	3.40	5.043	4.865	5.493	5.840	1.28	0.11678	0.22742
T_c	126	154.58	150.725	209.286	289.734	32.9	3.3099	5.1895
d_c	314	436.2	535	908	1110	31.4	41.45	69.6

*Indicates, following Levelt Sengers *et al.* [19], that the estimated parameters are of limited reliability.

that the molecular structure persists up to about 20 GPa: i.e. beyond the pressure at which the optical gap vanishes. The coexistence of the molecular and metallic states was stressed in the energy band calculations of Siringo *et al.* [23], which were designed to throw further light on the electrical transport measurements of Drickamer *et al.*.

Very recently, Fujihisa *et al.* [24] have performed structural studies of solid bromine subjected to high pressure using synchrotron radiation X-ray diffraction techniques in conjunction with a diamond-anvil high pressure cell. Intensity measurements in the molecular Br_2 phase were made up to 80 GPa, where solid bromine then exhibits a molecular to monatomic phase transition.

By combining their measurements on solid bromine with earlier results on iodine and chlorine, Fujihisa *et al.* propose an empirical scaling rule for crystal structure, scaled with the diatomic molecular bond length for the three isostructural solid halogens. Their use of the Herzfeld criterion also prompts them to propose a scaling law for the occurrence of coexisting metallic and molecular states; the precursor of molecular dissociation.

Briefly, on the first scaling law, the X-ray diffraction work of Fujii *et al.* [25] demonstrated that molecular dissociation in solid bromine occurs at 80 GPa. Using a scaled volume, $\tilde{v}$ say, which they define as $\tilde{v} = v/8R_b^3$ where $v = abc$ is the unit cell volume and R_b is the molecular bond length in the solid molecular phase, Fujihisa *et al.* [24] point out that, for both iodine and bromine, molecular dissociation results at $\tilde{v}_c = 1.29$. They conclude therefore that the bond length R_b is a relevant scaling parameter. The 'universal' behaviour in the scaled lattice constants versus $\tilde{v}$ was also noted by Fujii *et al.* [25].

Fujihisa *et al.* [24] also address the question as to whether any scaling regularities exist for the transition to a metllic phase prior to molecular dissociation. To explore this, they invoke the Herzfeld criterion [10]. In the Herzfeld phenomenology, the dimensionless parameter Rd/M is utilized, where R is the molar refractivity, M the molar weight and d the density. In the halogens R has the vlaues collected in Table III, the corresponding values of Rd/M being also recorded. Their Figure 7 shows the pressure dependence of Rd/M as calculated for the three halogens from the unit cell volume. These workers note that $Rd/M = 0.60$ at zero pressure for I_2 corresponds to that at 10 GPa for Br_2. The theoretical limit $Rd/M = 1$ for the metallic

TABLE III Molar refractivity R of halogens I_2, Br_2 and Cl_2 and corresponding values of Herzfeld parameter Rd/M (after Fujihisa *et al.* [24])

	I_2	Br_2	Cl_2
R	30.6	17.5	11.7
Rd/M at 0 GPa	0.60	0.44	0.34

phase to occur predicts then pressures required for I_2 and Br_2 of 21 and 80 GPa respectively. These predictions are close to the pressures required for molecular dissociation in both these cases.

Fujihisa *et al.* [24] conclude that (i) by combining data for I_2, Br_2 and Cl_2 a useful scaling rule is obeyed in the three isostructural halogens, with molecular dissociation occurring at the critical scaled volume $\tilde{v}_c = 1.29$; (ii) by applying the Herzfeld criterion, full metallization corresponding to $Rd/M = 1$ occurs also at $\tilde{v}_c = 1.29$. Gap closure is predicted to occur at $\tilde{v} = 1.37$.

It is relevant to add here that by a different theoretical approach, the pressure induced insulator-metal transition in nitrogen has been treated [26].

5. MELTING AND ORIENTATIONAL DISORDER

In early work by Grace and Kennedy [27] the melting curve of N_2 was measured, along with those of other molecular solids, up to ≈ 30 kbar (see also Crawford *et al.* [28]) .

5.1. Computer simulation and modelling: mainly N_2

Subsequently, serveral computer simulation studies of nitrogen have been carried out. These embrace the fluid equation of state over a wide range of pressure and temperature (see e.g. [29]), the structure in a low-temperature β-solid phase [30] and a study of the mechanisms for the transitions in the solid state at high pressures [31].

Meijer *et al.* [32] have reported the location of the melting point of nitrogen at 300 K by Monte Carlo simulation, using a well tested pair potential. They note that in the regime of pressures between 0.75 and 3.0 GPa, the densities for both solid and fluid phases are significantly lower than the experimental values reported by Mills *et al.* [33] and Schifert *et al.* [34, 35]. They attribute this to a need for a refined model potential.

We want to add some comments relating to melting and orientational disorder by referring to the modelling of the thermodynamic properties of the solid phase and solid-liquid phase equilibria of hard dumbbells. We cite here the investigation of Vega *et al.* [36] from which earlier references in this area can be built up. The focus of thier study was the stability of the orientationally disordered (plastic crystal) solid phase in relation to both other solid phases and to the fluid phase. They cite evidence that molecules like N_2, with relatively mild anisotropy, are favourable for the formation of a plastic crystal phase in N_2 and lead to freezing into an orientationally ordered phase.

5.2. Zig-zag chains in molecular I_2 and H_2

We shall return to orientational disorder below, in relation to the lighter halogens. However, to motivate what follows, we shall anticipate somewhat the discussion of secion 6 on detailed solid-solid phase transitions by reference to the work of Pasternak *et al.* [38] on solid molecular I_2. The upper part of Figure 2, constructed from their paper, shows the low-pressure molecular phase. The middle part of the Figure shows how, on compression, the linkage 1-2′ in the upper Figure leads to bonding into zig-zag chains of I_2. According to Pasternak *et al.*, this is a quasi one-dimensional structure. Further increase in pressure leads to the configuration shown in the lowest part of Figure 2, which has the character of a two-dimensional structure.

Before returning to melting and orientational disorder, we want to refer to the subsequent results of computer studies of Hohl *et al.* [39] on solid H_2, which, in parallel with the work of Pasternak *et al.* [38] on solid I_2 discussed above, were interpreted in terms of zig-zag chains of diatomic molecules.

With this background, and stimulated especially by the very recent model of Siringo [40] in which he has proposed a d-dimensional lattice model incorporating some degree of frustration and thereby capable of describing some properties of molecular orientation in appropriate molecular solids, Tozzini *et al.* [41] have utilized the phenomenology laid down by Pople and Karasz [42] (see also [43] and [44]). This generalizes the Lennard-Jones and Devonshire [45] approach to

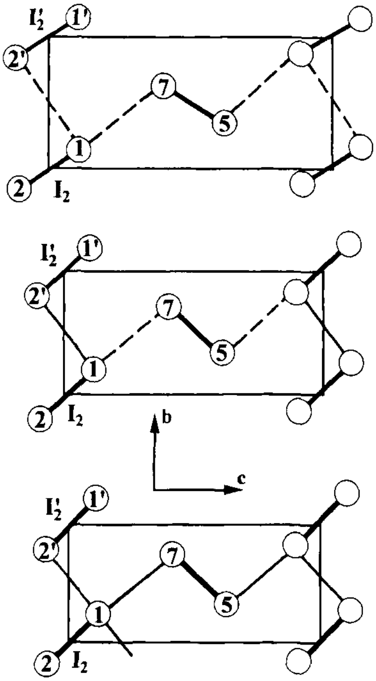

FIGURE 2 Schematic representation of the proposed elementary steps in the structural deformation of solid iodine under pressure (after Pasternak *et al.* [38]).

positional disordering (melting), based on the Bragg-Williams approximation to include the possibility of orientational disordering. Only two possible orientations, separated by an energy barrier, are considered for simplicity, the case of n orientations with $n > 2$ being treated subsequently by Amzel and Becka [44].

The Pople-Karasz phenomenology leads to a universal curve for the ratio T_m/T_c versus $1/T_c$ in suitable scaled units, T_m being the melting temperature and T_c the orientational disordering temperature. That T_m/T_c is a function of $1/T_c$ in the early model of fleixble molecules proposed by Longuet-Higgins [46] is also emphasized by Tozzini *et al.* [41].

5.3. Fluid nitrogen at high densities and temperatures

We refer here to the work of Nellis *et al.* [47], where dynamic equation of state data are given for liquid N_2 which has been subjected to single and double shock to pressures of 100 GPa, with compressions resulting in a fourfold increase in the liquid density and internal energies to 1 MJ/mole.

In Figure 1 of their paper, single-shock compression curves (Hugoniots) for liquid N_2 are compared with previous Hugoniot data on CO [48]. N_2 and CO are isoelectronic, have very similar critical points (see section 3 on N_2) and in the shock measurements had initial liquid density $\approx 0.89\ \mathrm{cm}^{-3}$ in each case. N_2 and CO follow the same curve, which is also understood theoretically [49] up to 15 GPa. Then the CO Hugoniot softens, which can be interpreted as due to chemical decomposition [48]. The Hugoniot curves come together again above about 70 GPa. Nellis *et al.* [49] conclude that above this pressure the fluids are compressed sufficiently that the atomic number density of the initial state essentially determines the $p-V$ curve.

For some interesting phenomenology related to the Hugoniots of nitrogen and carbon monoxide, the reader is referred to the study of Nellis *et al.* [49]. The review by Nellis [50] remains a good general reference in this area. It is also relevant in the present context to refer to the large anisotropy in the *ab initio* N_2–N_2 repulsive potential, which can vary by a factor of 100 depending on the angle of approach of two N_2 molecules [51]. This anisotropy is , for instance, about an order of magnitude larger than for H_2 [52].The studies on N_2 by Ross and Ree [53] and the molecular dynamics calculations by Johnson *et al.* [54] are also noteworthy.

5.4. Melting of O_2 and Orientational Correlations

Before closing this section, we shall record briefly some facts concerning the melting transition of O_2. The melting line was discussed by d'Amour *et al.* [55]. But what we shall focus attention on here is the change in the optical absorption of O_2 on melting. To this end Figure 3, taken from the study of Nicol and Syassen [56], compares the unpolarized optical absorption spectrum of O_2 in the liquid phase at 5.4 GPa with those in the crystalline β phase. We shall return to the crystalline curves, very briefly, in the next section of this review. What is noteworthy at this point is that there is a marked change in the integrated intensities of specfic bands, these intensities decreasing by a

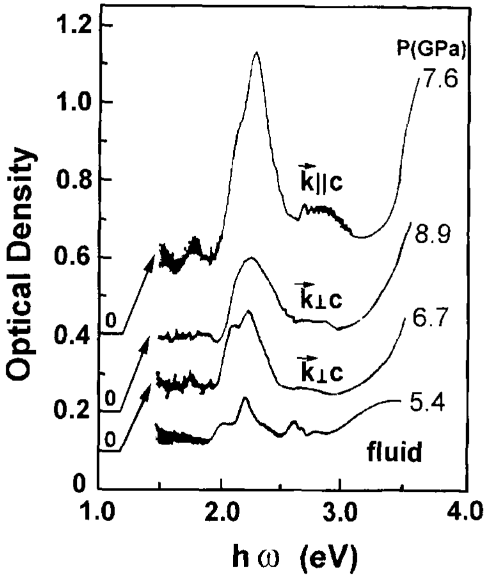

FIGURE 3 Unpolarized optical absorption spectra of O_2 in the fluid phase at 5.4 GPa and in the crystalline β phase (after Nicol and Syassen [56]).

factor of 5 in the fluid relative to the 7.6 GPa spectrum. Nicol and Syassen attribute this to the combination of reduced intermolecular orientational order and random orientation relative to the photon field. They also emphasize that in the fluid phase the spectral intensities vary with pressure to a greater extent as might be anticipated from the quadratic density dependence of these intensities as observed by Blickensderfer and Ewing [57] at low pressures. What is stressed by Nicol and Syassen is that changes in the orientational correlations between the solid and the dense fluid could be the explanation of the difference.

Following this section devoted largely to melting and to orientational features of assemblies of homonuclear diatomic molecules, we shall return in the penultimate section immediately below to relatively low temperature phases and to richer detail in the phase diagrams, predominantly though not exclusively at relatively low pressures.

6. LOW TEMPERATURE PHASES AND ELEMENTARY EXCITATIONS

6.1. Orientational Ordering in Solid Hydrogen

Mazin *et al.* [58] have very recently presented a unified view of orientational ordering. The summary below is based on their work.

They emphasize three regimes of orientational ordering. At the lowest pressures, as van Krankendonk reviews [59] the orientationally disordered hcp phase I and the cubic Pa3 phase of ortho-H_2/para-D_2 are fairly well understood. The important concept here is ordering of the angular momenta of individual molecules, due to quadrupolar interactions. The ordered phase is such that the axes of quantization are aligned along the body diagonals of an f.c.c cell: the lowest energy state for an assembly of quadrupoles.

As the pressure is increased, another type of ordering is found [60]: phase II, identified near 0 K and 22 GPa in ortho-D_2 [61] and at 110 GPa in para-H_2 [62]. Here, as Mazin *et al.* discuss, the ordering occurs even in the assembly of $J = 0$ molecules by virtue of a broken symmetry transition in which higher J levels form an admixture in the ground state resulting from enhanced intermolecular interactions. Ortho-para distinctions can be made, and a family of transitions exists as a function of ortho-para content. Since higher angular momenta enter the admixture in the ground state, both ortho and para molecules possess non-zero angular momentum and quadrupole moments which can exhibit orientational order.

As the pressure is increased further, a transition to a phase III has been observed, which spectroscopic data indicate to possess also orientational ordering [60, 62, 63]. As Mazin *et al.* emphasize, present understanding of this phase III is incomplete. However, experiment reveals the transition between the two orientationally ordered phases II and III as a much stronger change in the assembly than at the I-II boundary due to orientational ordering. Mazin *et al.* interpret the differences between the phases as due to quantum mechanical ordering in phase II, in contrast to classical ordering in phase III. These workers assert that the quantum-classical transition into phase III has important consequences for the evolution of ortho-para states with increasing pressure. For further details of both theory and experiment, the reader is referred to the account of Mazin *et al.* [58].

6.2. Phase Boundaries at low Temperature in Solid Halogens

The Japanese X-ray diffraction studies [22, 24], plus especially the Mössbauer spectroscopy of Pasternak *et al.* [38] lead to a picture of dimensionality changes with increasing pressure in I_2 (see the schematic illustration in Figure 2). As already discussed in section 5.2, pressure induces transitions from a molecular solid phase into a structure of zig-zag chains and then into a two-dimensional layer-like assembly. Evidence for dimensionality changes under pressure has also been presented for solid H_2 in the quantal simulation study of Hohl *et al.* [39]. Thus, some of the considerations to follow for solid iodine may apply also to solid hydrogen, though in a quite different pressure range for the two materials.

Bhatia *et al.* [64] (see also the book by March and Parrinello [65]) have discussed the way in which, at low temperature, phase boundary behaviour depends on the nature of the elementary excitations. This viewpoint is pressed qualitatively below in relation to dimensionality changes in solid I_2 under pressure.

Starting from the three-dimensional molecular solid I_2 at low T and p (phase 1 say), the dimensionality is lowered at the first phase transition by passing to filamentary zig-zag molecular chains (phase 2). It is known, for instance, in C that diamond at low temperature has specific heat $C_v \propto T^3$ whereas graphite has $C_v \propto T^2$. Thus the entropy S at low temperature is higher in the lower dimensional phase 2 and hence $S_1 - S_2$ in negative. Invoking the Clausius-Clapeyron equation

$$\frac{\Delta S}{\Delta V} = \frac{\partial p}{\partial T} \tag{6.1}$$

the sign of the slope of the T-p curve away from $T = 0$ is evidently determined, since $\Delta S = S_1 - S_2$ is negative, by the sign of ΔV. To our knowledge, this has not been determined experimentally in iodine.

However, as we pass from phase 2 to the layer-like phase 3, it seems clear that $\Delta S = S_2 - S_3$ will be positive. But $\Delta V = V_2 - V_3$, since pressure plus increased dimensionality should make the material more dense, should also be positive. Hence $\partial T / \partial p$ will be positive and tend to infinity as $T \rightarrow 0$. The extent of the largely non-interacting zig-zag chain phase should therefore be increased with increasing temperature in solid I_2, at least at low temperatures.

6.3. Optical Spectra of Solid Oxygen at High Pressure

We return at this point to a further discussion of optical absorption in the crystalline β phase of O_2 and in particular to the data of Nicol and Syassen [56] in Figure 3. The occurrence of three solid phases of oxygen near room temperature and the intense colours of these phases [66] distinguish O_2 from other diatomics. These are transparent in the visible and ultraviolet at similar pressures. One can thus study in oxygen the way in which compression of intermolecular separations can affect the electronic states of such a molecular solid. Figure 1 of the paper by Nicol and Syassen [56] shows the potential energy diagram of the O_2 molecular states relevant to their experimental study.

In Figure 3 of the present article, let us pick out first the spectrum shown at 7.6 GPa. This was obtained in the β phase with a crystal in which the c axis of the hexagonal unit cell was such that the light was propagating parallel to the axes of the O_2 molecules. In contrast, the c axis of the crystal on which the spectra shown at 6.7 and 8.9 GPa were measured was perpendicular to the propagation direction. Nicol and Syassen stress that five features can be isolated in one or more of the curves depicted in Figure 3. For full details the reader is referred to their account. One of these features is the weak, near-infrared ${}^1\Sigma_g^+ \leftarrow {}^3\Sigma_g^-$ band while another is the prominent $2^1\Delta_g \leftarrow 2^3\Sigma_g^-(O-O)$ band. These workers note that the $2^1A_g \leftarrow {}^3\Sigma_g^-$ band near 2 eV and the more intense vibronic band near 2.2 eV appear in all the spectra displayed in Figure 3. As the pressure is increased, these bands move to higher energies by approximately 0.03 eV/GPa. We have referred earlier to the changes of the integrated intensities of certain bands (especially the $2^1\Delta_g \leftarrow 2^3\Sigma_g^-$ bands) on melting. Such pressure measurements as those of Nicol and Syassen contain a wealth of information on the changes taking place in the electronic states as the intermolecular separations are reduced by pressure.

6.4. High Pressure Properties of Solid O_2

Helmy *et al.* [67] have calculated the static and dynamic properties of solid α-oxygen under pressure at $T=0$ using a pattern recognition optimization procedure and harmonic lattice dynamics. A variety of physical properties were studied, embracing lattice parameters, sound velocities, compressibility, phonon and libron dispersion curves, root means square translational and librational fluctuations and the pressure dependence of the intramolecular stretching mode.

One of the conclusions drawn by these authors is that the magnetic interaction influences the behaviour of the solid under pressure. They also predict, at $T=0$, a soft-mode induced phase transition from the monoclinic α structure to an orthorhombic structure at ≈ 6 kbar.

Following this work Meier *et al.* [4] have studied solid oxygen under pressure at low temperatures up to 60 kbar. In particular, as will be elaborated a little below, librons and vibrons were observed by means of Raman light scattering. These workers present evidence for a (weakly) first-order phase transition at about 9 kbar. Helmy *et al.* [67] had predicted a phase transition in this range of temperature and pressure. However, further theoretical work is required to bring experiment and theory into full accord.

Previous high-pressure studies using Raman light scattering were performed at high temperatures [66] (see also [68]). Meier *et al.* [4] report an extensive study of the low-energy excitations at low temperature. They note that the Raman spectrum of solid oxygen has three notable features at low pressure: (i) the vibron, which is a collective long-wavelength excitation of the intramolecular vibration, (ii) the libron and (iii) the so-called D band at near twice the energy of the single libron. In their work these excitations were investigated at both 6 K and 18 K for pressures up to 60 kbar. Observations could be made on the D band up to 35 kbar, beacuse of marked broadening at higher pressures. The main finding was that the linewidth of the libron band increases from 3 cm^{-1} at $p=0$ to about 12 cm^{-1} at 50 kbar, while the vibron width is less than 2 cm^{-1}. No appreciable differences were detected between the 6 K and 18 K measurements.

Though the absolute agreement between the theory of Helmy *et al.* [67] and the experiments is only modest, Meier *et al.* stress that Helmy *et al.* recognized uncertainties with respect to the intermolecular potential they employed. Such uncertainties could well be the reason for the differences between experiment and theory.

6.5. Solid N_2 Under Pressure

We refer elsewhere in this article to the insulator-metal transition under pressure in N_2. Here we summarize experimental optical studies of solid N_2 up to 130 GPa. In the experimental investigation of Reichlin *et al.* [69], high-resolution Raman spectroscopy was used to investigate phase changes in solid molecular nitrogen as pressure was increased in a region accessible to the diamond-anvil cell. These Raman scattering measurements revealed phase changes at 20, 66 and 100 GPa through branching exhibited by vibronic modes. There was no evidence for a transition to a metallic state over a pressure range up to 130 GPa. The data indicate that nitrogen retains its molecular character, notwithstanding the various phase transitions detected in the above regime of pressure.

However, Reichlin *et al.* [69] also make the point that it is not proved beyond doubt that the diatomic molecular form of solid nitrogen actually remains the stable species. They refer in this context to the theoretical study of McMahan and LeSar [70], which pointed out that crystalline forms composed of N_2 molecules could be less stable than a monatomic simple cubic structure at 0 K and from $\approx 80-95$ GPa. That molecular structures might remain metastable to considerably higher pressures was envisaged by McMahan and LeSar from their theoretical work.

Notwithstanding the above discussion, it is to be stressed that nitrogen in the predicted metallic simple cubic or A7 rhombohedral structures has not been observed experimentally in the pressure range up to 130 GPa. Reichlin *et al.* [69] comment that the three phases observed in their experiments appear to be described as distortions of the Pm3n cubic structure (see also Schifert *et al.* [71]), and conjecture that the formation of superlattices may be involved.

6.6. Insulator-metal Transition in Hydrogen (Deuterium) Briefly Revisited

In the examples discussed earlier in this section, one is in ranges of pressure and temperature which are now accessible to controlled experiments in the laboratory. To finish this section, we shall briefly return to the shock compression experiment of Weir *et al.* [11] on hydrogen and deuterium. There, in the liquid phase, a coexisting metallic and molecular state was observed at pressure of $\approx$ 1.8 Mbar. Their speculation was that a substantially higher pressure would be required to induce a corresponding insulator-metal molecular phase transition in the cold solid.

This can, at least qualitatively, be understood in terms of elementary excitations. We expect the entropy of the metallic state at low temperature, involving single electron excitations, to vary linearly with temperature and to exceed that of the insulating state. Also the specific volume of the insulating state can be anticipated to be greater than that of the metallic state and hence from the Clausius-Clapeyron equation (6.1), $\partial T/\partial p$ will be negative, becoming infinite in magnitude as T tends to zero. In contrast to the I_2 example above, the extension of the metallic phase as a function of pressure will, at least at low temperature, be reduced as T increases.

7. SUMMARY AND FUTURE DIRECTIONS

That pressure is a most valuable tool for exploring aspects of the physics and chemistry of condensed phases of assemblies of the homonuclear diatomic molecules considered here cannot fail to be recognized, from the admittedly selected topics in this short review. Both laboratory experiments using the diamond anvil cell, and shock measurements, have contributed hugely to our understanding of the general area reviewed here. The richness of the phase diagram exposed for what might appear to be a simple substance, namely condensed N_2 is already evident from available experiments and theory, although much remains to be done. For instance though theory points to the fact that cold solid nitrogen should undergo a transition to a metallic state in an accessible range of pressure for available laboratory techniques, this does not appear, so far, to have been unambiguously achieved. However, clearcut insulator-metal transitions, passing initially through coexisting molecular and metallic states are now well established for the solid halogens I_2 and Br_2.

Solid oxygen, with its rather unique optical and magnetic properties, offers scope for further investigation, with particular emphasis to be placed on the interplay between spin-independent and magnetic interactions referred to earlier. There also appears to be room for further interesting work, both experiment and theory, on the way the elementary magnetic excitations in the antiferromagnetic solid affect the shape of the phase boundaries at low temperature.

Of course, in many respects the 'jewel in the crown' remains to detect in cold solid hydrogen a clearcut transition into a metallic phase. Ever since the pioneering studies of Wigner and Huntington this are has remained of central interest to researchers working in both theory and experiment in the area of the physics and chemistry of condensed molecular systems under extreme conditions of pressure.

Acknowledgements

The contribution of one of us (NHM) to this article was brought to fruition during a stay at the Scuola Normale Superiore di Pisa. NHM wishes to thank the Scuola for generous hospitality. He is greatly indebted to Professor R. Pucci and his colleagues in the University of Catania for much collaboration and stimulation on problems embraced by the present review.

References

[1] Young, D. A., *Phase Diagrams of the Elements* (University of California, Berkeley 1991).

[2] Pilgrim, W.-C., Winter, R. and Hensel, F. (1993). *J. Phys.: Condens. Matter.*, **5**, B183.

[3] Bondi, A., *Physical Properties of Molecular Crystals, Liquids and Glasses* (Wiley, New York 1968).

[4] Meier, R. J., Van Albada, M. P. and Lagendijk, A. (1984). *Phys. Rev. Lett.*, **52**, 1045.

[5] Meier, R. J., Schinkel, C. J. and De Visser, A. (1982). *J. Phys.*, **C15**, 1015.

[6] Stephens, P. W., Birgenau, R. J., Majkrzak, C. F. and Shirane, G. (1983). *Phys. Rev.*, **B 28**, 452.

[7] Meier, R. J. and Helmholdt, R. B. (1984). *Phys. Rev.*, **B 29**, 1387.

[8] Ross, M. and McMahan, A. K. in *Physics of Solids under Pressure*, eds. Schilling, J. S. and Shelton, R. N. (North-Holland, Amsterdam 1981) p. 161.

[9] Leung, W. B., March, N. H. and Motz, H. (1976). *Phys. Lett.*, **56A**, 425.

[10] Herzfeld, K. F. (1927). *Phys. Rev.*, **29**, 701.

[11] Weir, S. T., Mitchell, A. C. and Nellis, W. J. (1996). *Phys. Rev. Lett.*, **76**, 1860.

[12] Magro, W. R., Ceperley, D. M., Pierleoni, C. and Bernu, B. (1996). *Phys. Rev. Lett.*, **76**, 1240.

[13] March, N. H. and Tosi, M. P. (1996). *N. Cimento*, **18D**, 1061.

[14] Stishov, S. M. (1975). *Soviet Physics Uspekhi*, **17**, 625.

[15] March, N. H., Perrot, F. and Tosi, M. P., to be published.

[16] Blinder, S. M., *Advanced Physical Chemistry* (Macmillan, London 1969).

[17] Guggenheim, E. A. (1945). *J. Chem. Phys.*, **13**, 253.

[18] Berry, R. S., Rice, S. A. and Ross, J., *Physical Chemistry* (Wiley, New York 1980).

[19] Levelt Sengers, S. M. H., Greer, W. L. and Sengers, J. V. (1976). *J. Phys. Chem. Ref. Data.*, **5**, 1.

[20] Drickamer, H. G. (1965). *Solid State Physics*, **17**, 1; Drickamer, H. G., Lynch, R. W., Clendenen, R. L. and Perez-Albuerne, L., (1966). ibid. **19**, 135.

[21] Riggleman, B. M. and Drickamer, H. G. (1963). *J. Chem. Phys.*, **38**, 2721.

[22] Shimomura, O., Takemura, K., Fujii, Y., Minomura, S., Mori, M., Noda, Y. and Yamada, Y. (1978). *Phys. Rev.*, **B 18**, 715.

[23] Siringo, F., Pucci, R. and March, N. H. (1988). *Phys. Rev.*, **B 37** 2491; ibid., **38**, 9567.

[24] Fujihisa, H., Fujii, Y., Takemura, K. and Shimomura, O. (1995). *J. Phys. Chem. Solids*, **56**, 1439.

[25] Fujii, Y., Hase, K., Ohishi, Y., Fuhihisa, H., Hamaya, N., Takemura, K., Shimomura, O., Kikegawa, T., Amemiya, Y. and Matsushita, T. (1989). *Phys. Rev. Lett.*, **63**, 536.

[26] Helmy, A. A. (1994). *J. Phys.: Condens. Matter*, **6**, 985.

[27] Grace, J. D. and Kennedy, G. C. (1967). *J. Phys. Chem. Solids*, **28**, 977.

[28] Crawford, R. K., Daniels, W. B. and Cheng, V. M. (1975). *Phys. Rev.*, **A 12**, 1690.

[29] Belak, J., Etters, R. D. and LeSar, R. A. (1988). *J. Chem. Phys.*, **89**, 1625.

[30] Klein, M. L., Levesque, D. and Weis, J. J. (1981). *J. Chem. Phys.*, **74**, 2566.

[31] Nosé, S. and Klein, M. L. (1983). *Phys. Rev. Lett.*, **50**, 1207; *Mol. Phys.*, **50**, 1055.

[32] Meijer, E. J., Frenkel, D., LeSar, R. A. and Ladd, A. J. C. (1990). *J. Chem. Phys.*, **92**, 7570.

[33] Mills, R. L., Liebenberg, D. H. and Bronson, J. C. (1975). *J. Chem. Phys.*, **63**, 1198.

[34] Schifert, D., Cromer, D. T. and Mills, R. L. (1978). *High Temp. High Press.*, **10**, 493.

[35] Schifert, D., Cromer, D. T., Ryan, R. R., Larson, A. C., LeSar, R. A. and Mills, R. L. (1983). *Acta Crystall.*, **C 39**, 1151.

[36] Vega, C., Paras, E. P. A. and Monson, P. A. (1992). *J. Chem. Phys.*, **97**, 8543.

[37] Singer, S. J. and Mumaugh, R. (1990). *J. Chem. Phys.*, **93**, 1278.

[38] Pasternak, M., Farrel, J. N. and Taylor, R. D. (1987). *Phys. Rev. Lett.*, **58**, 575.

[39] Hohl, D., Natoli, V., Ceperley, D. M. and Martin, R. M. (1993). *Phys. Rev. Lett.*, **71**, 541.

[40] Siringo, F. *Phys. Lett.*, A (in press).

[41] Tozzini, V., March, N. M. and Tosi, M. P., to be published.

[42] Pople, J. A. and Karasz, K. E. (1961). *J. Phys. Chem. Solids*, **18**, 28; ibid., **20**, 1295.

[43] Smith, G. W. (1965). *J. Chem. Phys.*, **42**, 4229.

[44] Amzel, L. M. and Becka, L. N. (1969). *J. Phys. Chem Solids*, **30**, 521.

[45] Lennard-Jones, J. E. and Devonshire, A. F. (1939). *Proc. Roy. Soc.*, **A 169**, 317; ibid., A **170**, 464.

[46] Longuet-Higgins, H. C. (1958). *Disc. Faraday Soc.*, **25**, 86.

[47] Nellis, W. J., Holmes, N. C., Mitchell, A. C. and van Thiel, M. (1984). *J. Chem. Phys.*, **53**, 1661.

[48] Nellis, W. J., Ree, F. H., van Thiel, M. and Mitchell, A. C. (1981). *J. Chem. Phys.*, **75**, 3055.

[49] Nellis, W. J., Holmes, N. C., Mitchell, A. C. and van Thiel, M. (1984). *Phys. Rev. Lett.*, **53**, 1661.

[50] Nellis, W. J. in *Shock Waves in Condensed Matter - 1983*, eds Asay, J. R., Graham, R. A. and Straub, G. K. (Elservier, New York 1984), p. 31.

[51] Ree, F. H. and Winter, N. W. (1980). *J. Chem. Phys.*, **73**, 322.

[52] Ree, F. H. and Bender, C. F. (1979). *J. Chem. Phys.*, **71**, 5362.

[53] Ross, M. and Ree, F. H. (1980). *J. Chem. Phys.*, **73**, 6146.

[54] Johnson, J. D., Shaw, M. S. and Holian, B. L. (1984). *J. Chem. Phys.*, **80**, 1279.

[55] d'Amour, H., Holzapfel, W. B. and Nicol, M. (1981). *J. Phys. Chem.*, **85**, 131.

[56] Nicol, M. and Syassen, K. (1983). *Phys. Rev.*, **B 28**, 1201.

[57] Blickensderfer, R. P. and Ewing, G. E. (1969). *J. Chem. Phys.*, **51**, 5284.

[58] Mazin, I. I., Hemley, R. J., Goncharov, A. F., Hanfland, M. and Mao, H. K. in press.

[59] van Krankendonk, J., *Solid Hydrogen* (Plenum, New York 1983).

[60] Mao, H. K. and Hemley, R. J. (1994). *Rev. Mod. Phys.*, **66**, 671.

[61] Silvera, I. F. and Wijngaarden, R. J. (1981). *Phys. Rev. Lett.*, **47**, 39.

[62] Lorenzana, H. E., Silvera, I. F. and Goettel, K. A., *Phys. Rev. Lett.*, **63**, 2080 (1989); ibid., **64**, 1939 (1990).

[63] Hemley, R. J. and Mao, H. K., *Phys. Rev. Lett.*, **61**, 857 (1988); ibid., **63**, 1393 (1989).

[64] Bhatia, A. B., Leung, W. B. and March, N. H. (1976). *Phys. Lett.*, **58A**, 205.

[65] March, N. H. and Parrinello, M., *Collective Effects in Solids and Liquids* (Hilger, Bristol 1982).

[66] Nicol, M., Hirsch, K. R. and Holzapfel, W. B. (1979). *Chem. Phys. Lett.*, **68**, 49.

[67] Helmy, A., Kobashi, K. and Etters, R. D. (1984). *J. Chem. Phys.*, **80**, 2782.

[68] Syassen, K. and Nicol, M., in *Physics of Solids under High Pressure*, eds J. S. Schilling and R. N. Shelton (North-Holland, Amsterdam 1981).

[69] Reichlin, R., Schifert, D., Martin, S., Vanderborgh, C. and Mills, R. L. (1985). *Phys. Rev. Lett.*, **55**, 1464.

[70] McMahan, A. K. and LeSar, R. (1985). *Phys. Rev. Lett.*, **54**, 1929.

[71] Schifert, D., Buchsbaum, S. and Mills, R. L. (1985). *J. Phys. Chem.*, **89**, 2324.